

FOPID controlled PV based QBC fed gamma Z-source inverter applicable for pump operations in an induction motor drive

Krishnan Selvaraj¹, Anbarasi Jebaselvi Gnanaiah David², Rama Reddy Sathi³, Pradeepa Kuppusamy³

¹Department of Electrical and Electronics Engineering, Sathyabama Institute of Science and Technology, Chennai, India

²Department of Electronics and Communication Engineering, Sathyabama Institute of Science and Technology, Chennai, India

³Department of Electrical and Electronics Engineering, Rajalakshmi Engineering College, Chennai, India

Article Info

Article history:

Received Mar 24, 2023

Revised Jun 11, 2023

Accepted Jun 25, 2023

Keywords:

FOPID controller

Gamma Z-source inverter

Induction motor

PI controller

Quadratic boost converter

ABSTRACT

A closed loop current mode-fractional-order-PID (CM-FOPID) controlled and PV based quadratic-boost-converter (QBC) fed gamma Z-Source Inverter with Induction motor system (PV-QBC-GZSI-IMS) for pump operation is proposed here. This work recommends a combination of QBC with gamma Z-source-inverter between the DC link source and asynchronous motor system. This will reduce the voltage rating of PV panel and its initial cost. GZSI reduces the current spikes in stator current. The objective of this research work is to regulate the speed of PV-QBC-GZSI-IMS. This effort deals with the closed loop response of PV-QBC-GZSI-IMS accompanied by current-mode-proportional integral (CM-PI) and CM-FOPID controllers. The performance investigations are analyzed with the control of QBC fed Gamma Z-source inverter with motor load using CM-PI and CM-FOPID controllers and the detailed comparison has been presented. MATLAB/Simulink outputs obtained with their respective speed and torque characteristics in time domain have been depicted. The closed loop CM-FOPID control of PV-QBC-GZSI-IMS is superior to the closed loop CM-PI control of PV-QBC-GZSI-IMS. The proposed QBC-converter reduces the voltage rating of PV panel and GZSI reduces current spikes in motor. The novelty of the article is to enhance the dynamic response of PV-QBC-GZSI-IMS using FOPID. The steady state error in torque is reduced to 0.52 N-m using FOPID.

This is an open access article under the [CC BY-SA](https://creativecommons.org/licenses/by-sa/4.0/) license.



Corresponding Author:

Krishnan Selvaraj

Department of Electrical and Electronics Engineering, Sathyabama Institute of Science and Technology
Chennai, India

Email: krishna05me@gmail.com

1. INTRODUCTION

The induction motor is popular for variable speed applications because it is more cost-efficient. The voltage rating of induction motor does not match with the voltage rating of PV. Hence a boost converter may be used between PV and induction motor. Various controllers with different modes of control have been taken into study and the summarizations of all those research results were compared and the net outcomes were shortlisted here. The hysteresis and PI current controllers, which control the load current, have problems with current ripple and phase lag, respectively.

The above problems are successfully handled by the suggested predictive current control technique [1]. Reduced steady state error and improved time domain responsiveness are two advantages of the FLC controlled cascaded fly back converter (CFLB) technology [2]. Utilizing the MATLAB-Simulink platform and the new European driving cycle (NEDC) test, the suggested controller's speed tracking capability is evaluated. "When compared to fuzzy FOPID controllers based on the genetic algorithm (GA) and particle

swarm optimization (PSO), the suggested controller provides the best performance for speed tracking” in [3]. The use of n-conventional converters is one possible solution to this problem; however, the complex control circuitry is required. An n-stage cascade converter in addition to a single active switch is an alternative solution [4]. A fuel-cell stack is modeled using electrical parameters. After that, the model is combined with a high step-up voltage converter model to create an integrated model that takes the behavior of the fuel-cell stack into account in [5]. “The suggested controller's inner loop is established on sliding-mode control, with a sliding surface established for the input inductor current. In an outer loop, a proportional-integral (PI) compensator that acts across the output voltage error adjusts the current reference value of the sliding surface obtained” in [6]. The MATLAB state flow toolbox and an NI data collecting system are used in the actual development of FOPID and IOPID controllers. The FOPID controller has improved performance and robust stability against the experiment variables, according to the results of the robustness study in [7]. While offering the same voltage boost, it may significantly reduce Z-source capacitor voltage stress and has an internal restriction on inrush current at startup [8]. It provides a larger boost capability, a broader input/output voltage range, and soft-switching capabilities without the use of extra components [9]. A Z-source inverter system implemented in [10]. Diode front ends are equipped with a tiny capacitor on the AC side and a unique LC network in the DC-link.

The current study aims to improve the dynamic responsiveness of the LCMI system by using an HC controller. As a result of the proposed LCMI system [11], a high voltage gain and enhanced time responsiveness can be achieved. In this study, we present a novel H10 inverter scheme for 2-level, 3-phase inverter applications. In the proposed architecture, CMV can be constant or zero without additional passive components [12]. An inverter built around a Z-source inverter (ZSI) with a grid-connected wind power production system. Based on the analysis of ZSI operation, a system for double closed-loop control is proposed [13]. To increase the controller's capabilities, a discrete-time model is implemented using the MPC technique. Using the controller, each phase current can be managed separately, enhancing system flexibility [14]. A hybrid model can be utilized as a numerical simulator for multi-source renewable energy systems (MS-RES). The model is simple and low-cost tool for constructing, validating, and assessing the outcomes of control techniques designed for energy transfer optimization in [15]. A linked transformer and fewer components are required for the proposed inverters when compared to existing topologies [16]. There is a double-frequency power imbalance between the dc input and ac output in single-phase photovoltaic (PV) systems. The passive network must buffer the energy of the double-frequency ripple (DFR). The suggested control method can greatly lower the capacitance required and produce low input voltage DFR without the use of any additional hardware components [17]. Adaptive control of ZSI is illustrated in [18]. A charging/discharging system that consists of a Cuk converter and a new controller to adjust the voltage of a dc-bus, The Cuk converter ensures system stability and rapid dynamic response for all working circumstances, while the controller ensures constant currents for the battery and dc-bus [19]. SM controllers provide higher transient performance than both regular PIDs and fractional-order PIDs (FOPIDs). In order to assess the efficiency of the SM controller, different time-domain criteria were used [20]. The inner loop of the suggested method is determined by the input inductor current control. The sliding manifold's reference signal is modified via an outside loop that regulates the output current. The Routh–Hurwitz criteria and the analogous control technique are used to determine the stability of two-loop controllers [21]. Protecting three-phase induction motors operating in single-phase mode is the focus of this dissertation using microcontrollers, GSM modules, step-down transformers, and protective relays [22]. A method for grid-connected cascaded multilevel 3-phase inverters that uses fuzzy logic. Current controllers and carriers used for traditional modulation have been totally eliminated by this approach [23]. Speed controller of 3 IM without PWM technology was used to evaluate the performance of the recommended controller under both constant and changing load conditions [24]. The suggested optimal PI and the regular PID are used to manage how the second DC-DC converter is used for battery charging [25]. This work aims to identify combination of suitable boost converter and inverter for induction motor fed pumps. This work also tries to improve the dynamic response of PV-QBC-GZSI-IMS.

The methodology flow chart is shown in Figure 1. Research problem is formulated based on literature survey on IM drives. After selecting converter and inverter, design calculations are made. Simulation of closed loop PV-QBC-GZSI-IMS with PI and FOPID are performed to identify better controller in closed loop. Comparison of related literature [10], [11] and proposed work on IMS is given in Table 1. The overview of this complete literature does not deal with PV-QBC-GZSI-IMS. This research suggests combination of QBC & GZSI to control IMS. The above literatures do not report the speed regulation of PV-QBC-GZSI-IMS using CM-FOPID controller. This work proposes CM-FOPID to control QBC-GZSI-IMS.

Our paper focuses on the identification of a non-isolated high gain DC-DC converter that has high voltage gain, a wide range of operation, and reduced input current ripples suitable for induction motor drive. Section 2 gives an overview of quadratic boost converter. Section 3 presents analysis of QBC-GZSI, section 4 gives description of QBC-GZSIS, section 5 provides simulation studies and comprehensive comparison of the simulation with PI and FOPID controllers, section 6 includes conclusion and future scope of work.

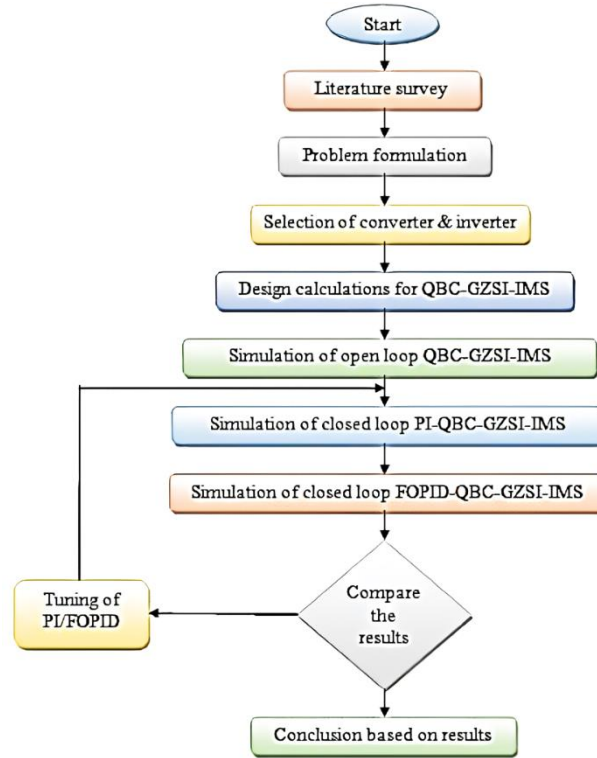


Figure 1. Methodology flow chart for QBC-GZSI-IMS

Table 1. Comparison of literature and our proposed work

Parameter	Existing Work by Peng [10]	Existing Work by Narendran and Sureshkumar [11]	Proposed work
No of stages	2	3	2
No of loops	Zero	2	2
Control method	Open loop control	Fopid	Fopid
Load	Three phase induction motor	Single phase induction motor	Three phase induction motor
Performance parameters	NA	Tp = 3.3 secs Ts = 3.6 secs	Tp = 3.29 secs Ts = 3.45 secs

2. QUADRATIC BOOST CONVERTER - AN OVERVIEW

A quadratic boost converter is a DC-DC boost converter with a second phase that boosts DC voltage. A quadratic boost converter output voltage is always larger than the input voltage. The output voltage may be calculated using the (1).

$$V_{OUT} = \frac{V_{IN}}{(1-D)^2} \tag{1}$$

MOSFETs (Q) serve as switches, while inductors (L), diodes (D), capacitors (C), and resistors (R) serve as loads in the quadratic boost converter (QBC) circuit depicted in Figure 2. The circuit will operate based on the assumption. If the switch is in ideal the capacitors C1 & C2 are considered to be large value and the voltage on the capacitors VC1 and VC2 is approximately stable throughout the switching process.

The (2) is used to calculate the gate current in the MOSFET, where PG is the power at the gate, VGS is the voltage at the input (VG) multiplied by the duty cycle % . (D).

$$I_G = \frac{P_G}{V_G} \tag{2}$$

Where

$$P_G = F_s Q_G V_{GS}; V_{GS} = V_G D \tag{3}$$

$$L = \frac{(1-D)^2 D R}{2fs} \tag{4}$$

$$C_1 = \frac{IoD}{(1-D)\Delta Vc1 fs} \tag{5}$$

$$C_2 = \frac{IoD}{\Delta Vc2 fs} \tag{6}$$

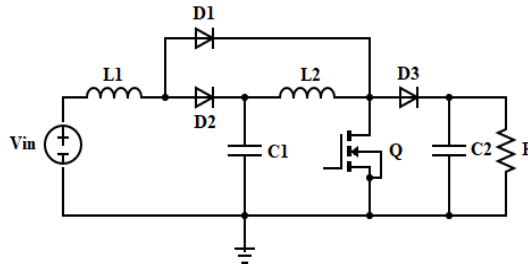


Figure 2. Quadratic boost converter circuit

3. ANALYSIS OF QBC-GAMMA ZSI SYSTEM

First two out of seven operating stages of PV-QBC-GZSI are explained here:

i) Stage-I: Charging circuit of stage-I is shown in Figure 3. The equations are as follows:

$$V_{C1} + V_{L2} = 0 \tag{7}$$

$$V_{in} = V_{L1} + V_{C1} \tag{8}$$

Where V_{in} is input voltage, V_{L1} and V_{L2} are voltage across L_1 and L_2 .

$$V_{an} = V_G/2 \tag{9}$$

$$V_{bn} = -V_G/2 \tag{10}$$

V_{an} and V_{bn} are voltage across phase a and phase b.

ii) Stage-II: Discharging circuit of stage-II is shown in Figure 4. When Q is turned off, energy in C_1 is transferred to C_2 . Then the energy in C_2 is transferred to C_3 . When S1 and S6 of GZSI are turned on, two phases of the load will receive the power. L_3 , L_4 and C_4 in GZSI will act as filters it will reduce the current spikes in stator current. The equations are as follows:

$$V_{in} = V_{L1} + V_{C1} \tag{11}$$

$$V_{C1} + V_{L2} = V_{C2} \tag{12}$$

$$V_{an} = V_G/2 \tag{13}$$

$$V_{bn} = -V_G/2 \tag{14}$$

The stages III to VII similar to stage-II with sequence of 12, 23, 34, 45, 56.

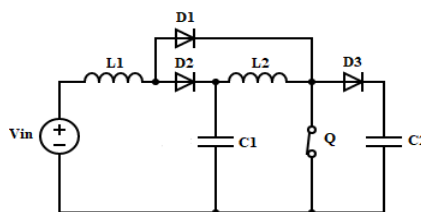


Figure 3. Stage-I: Charging circuit

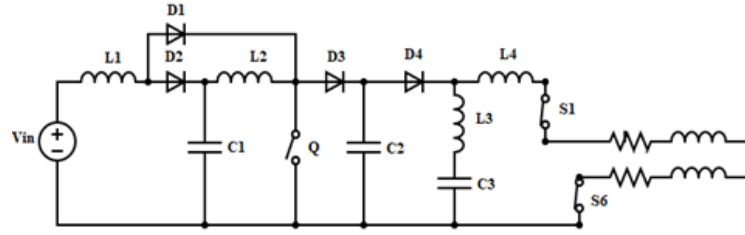


Figure 4. Stage-II - S1 and S6 ON

4. DESCRIPTION OF PROPOSED METHOD

Output of PV is used to charge the battery. Constant voltage from battery is stepped-up using QBC. The output of QBC is inverted and applied to 5HP-IM. Control unit of GZSI-IM is used to apply pulses to QBC & GZSI. Block structure of closed loop PV-QBC-GZSI-IMS using CM-PI and CM-FOPID-controller is delineated in Figure 5. Speed of 3 phase induction motor is sensed then it is compared with the reference speed to obtain speed error (SE). The SE is applied to speed PI/FOPID-1. The output of PI/FOPID-1 is compared with actual current and error is applied to PI/FOPID-2. The output updates the duty cycle of the QBC.

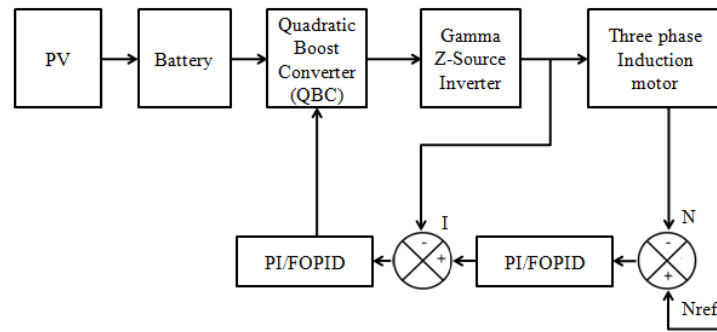


Figure 5. Block diagram of closed loop PV-QBC-GZSI-IMS using CM-PI and CM-FOPID Controller

4.1. FOPID Controller

Academics and industry have both been interested in FOPID controllers in recent years. In fact, they are more versatile than ordinary PID controllers (since they have five parameters to choose from), because they have five parameters to choose from. This may, however, make tuning the controller more difficult.

$$V_o(s) = K_p E + K_i \frac{E}{s} + K_D s^{\lambda} E \text{ for general PID-controller} \tag{15}$$

$$T_i C_{FOPID}(S) = K_p + \frac{K_i}{s^{\lambda}} + K_D s^{\mu} \tag{16}$$

4.2. Design considerations

The following assumptions were made to design QBC-GZSI-IMS is given in Table 2. From $V_{OUT} = \frac{V_{IN}}{(1-D)^2}$, D works out to 0.65. T_{ON} works out to 0.13 ms and T_{OFF} works out to 0.07 ms. $L = \frac{(1-D)^2 D R}{2fs}$; L works out to 0.02 mH. $C_1 = \frac{I_o D}{(1-D)\Delta V_{c1} fs}$; C1 works out to 1µF. $C_2 = \frac{I_o D}{\Delta V_{c2} fs}$; C2 works out to 9000 µF.

Table 2. Assumptions to design QBC-GZSI-IMS

Parameter	Value
Switching frequency (F _s)	5 kHz
Input voltage (V _i)	48 V
Output voltage (V _o)	400 V
Change in capacitor voltage (ΔV _{c2})	0.1
Resistor (R)	2.5Ω

5. SIMULATION RESULTS

Closed loop simulation of CM-PI and CM-FOPID controlled PV based QBC fed GZSI with induction motor in the MATLAB/Simulink is performed. The results are compared in terms of time domain parameters of speed in QBC-GZSI-IM. A better controller for QBC-ZSI-IM system is identified based on simulation results. Speed and torque response are obtained for a step change in input voltage using current- mode PI and FOPID controllers.

5.1. Closed loop CM-PI control PV based QBC fed GZSI with induction motor

The circuit diagram of Closed-loop- CM-PI control PV-QBC-GZSI-IMS is delineated in Figure 6. Speed signal is sensed then it is compared with reference speed. The SE is given to PI-1. Output of PI-1 is compared with current signal and CE is applied to PI-2. The output of PI-2 is used to update duty ratio of MOSFET in QBC. Triggering pulses of inverter, line voltage of motor, speed, torque and mechanical power are measured using scopes. Input-voltage of closed-loop-CM-PI control PV-QBC-GZSI-IMS is represented in Figure 7 and its value is 74 V. A source disturbance of 20% is applied at $t = 3.2$ secs.

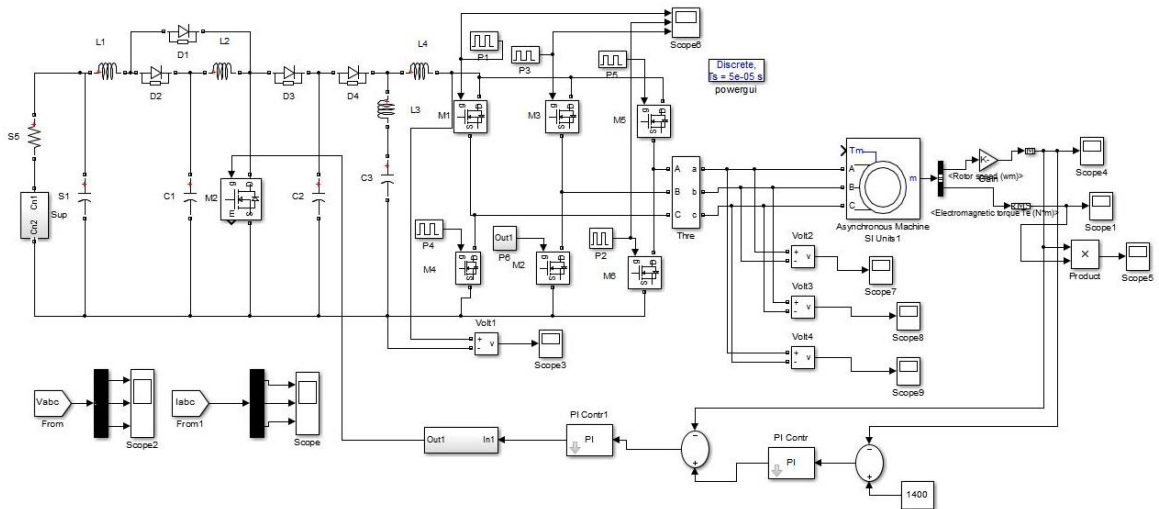


Figure 6. Simulation of CM-PI controlled PV-QBC-GZSI-IMS in MATLAB/Simulink

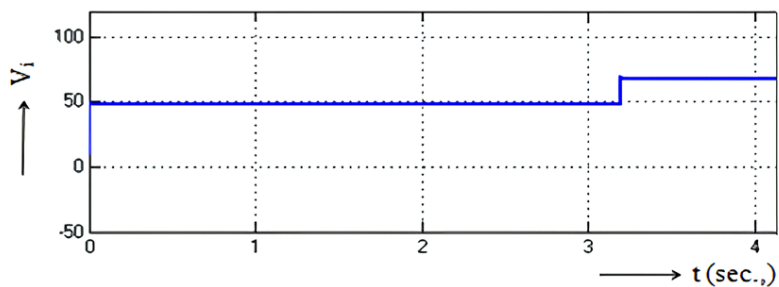


Figure 7. Input voltage of CM-PI controlled PV based QBC fed GZSI with IM

5.2. Closed loop CM-FOPID control PV based QBC fed GZSI with induction motor

The time response of PV-QBC-GZSI-IMS with CM-PI is sluggish. Hence it is proposed to control PV-QBC-GZSI-IMS using CM-FOPID controller. The circuit diagram of Closed-loop-CM-FOPID control PV-QBC-GZSI-IMS is delineated in Figure 8. Scopes are connected to display switching pulses, output of QBC, speed of IMS and torque of IMS.

Comparison curves for motor speed of Closed-loop- PV-QBC-GZSI-IMS is with CM-PI and CM-FOPID is delineated in Figure 9. The speed of PV-QBC-GZSI-IMS settles after few oscillations. Torque-response of Closed-loop- CM-PI and CM-FOPID control PV-QBC-GZSI-IMS is delineated in Figure 10. The torque of IMS settles without any oscillations. The motor speed with CM-FOPID is found to be less than that of CM-PI controlled PV-QBC-GZSI-IMS. The torque with CM-PI is higher than that of CM-FOPID controlled PV-QBC-GZSI-IMS.

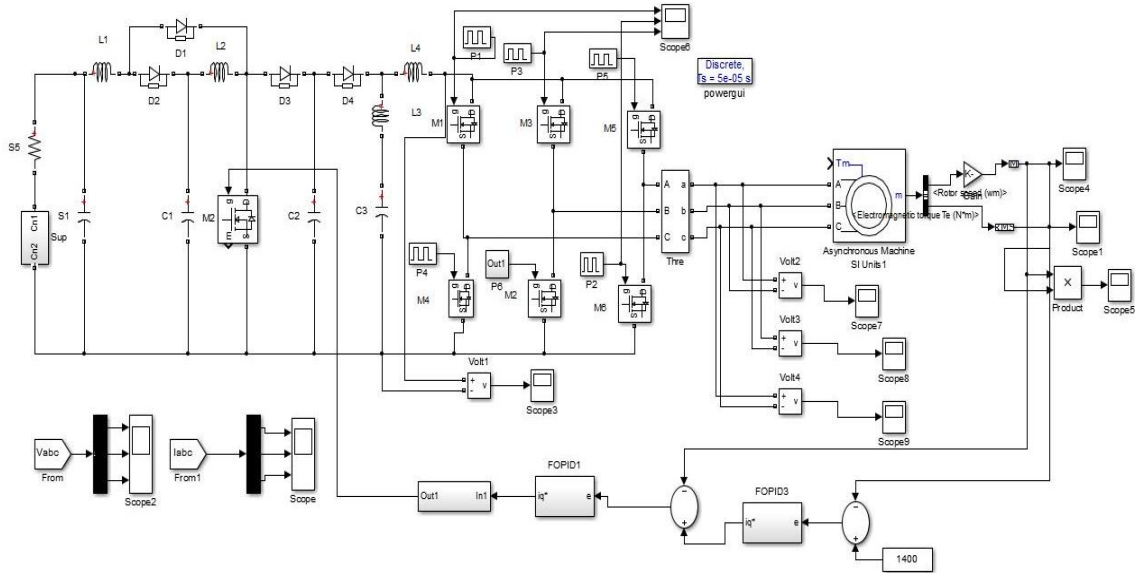


Figure 8. Simulation of CM-FOPID controlled PV-QBC-GZSI-IMS in MATLAB/Simulink

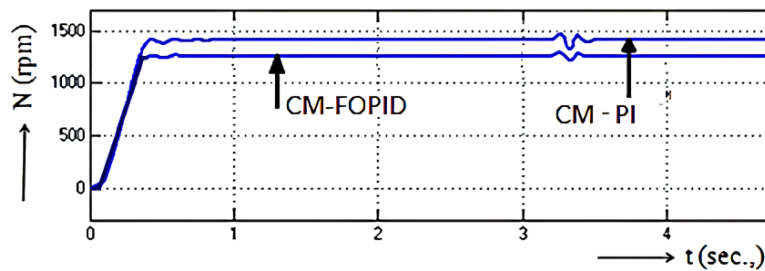


Figure 9. Motor speed of CM-PI and CM-FOPID Control PV-QBC-GZSI-IMS

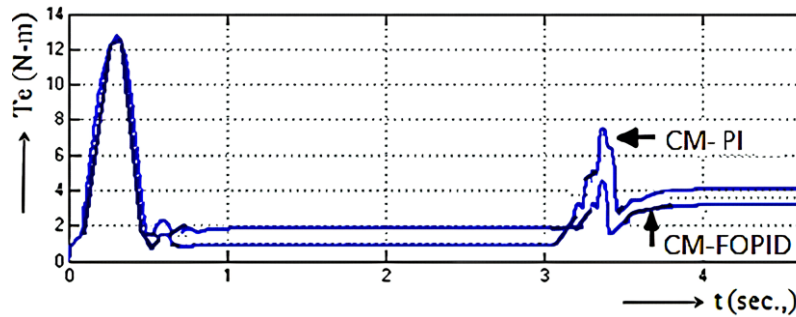


Figure 10. Motor torque of CM-PI and CM-FOPID control PV-QBC-GZSI-IMS

5.3. Comparison of time domain parameters of CM-PI and CM-FOPID control PV-QBC-GZSI-IMS

Table 3 outlines the time domain parameters for speed of 1300 RPM using CM-PI and CM-FOPID controller. By using CM-FOPID controller, rise-time is dwindled from 3.28 sec to 3.27 sec, peak-time is dwindled from 3.46 sec to 3.38 sec, settling-time is dwindled from 3.68 sec to 3.56 sec, steady-state-error is dwindled from 3.98 RPM to 2.85 RPM. Table 4 outlines the time domain parameters for torque with reference speed of 1300 RPM using CM-PI and CM-FOPID controller. By using CM-FOPID controller, rise-time is dwindled from 3.39 sec to 3.37 sec, peak-time is dwindled from 3.48 sec to 3.45 sec, settling-time is dwindled from 3.89 sec to 3.76 sec, steady-state-error is dwindled from 0.76 to 0.65 N-m.

Table 5 outlines the time domain parameters for speed of 1350 RPM using CM-PI and CM-FOPID controller. By using CM-FOPID controller, rise-time is dwindled from 3.27 sec to 3.26 sec, peak-time is

dwindled from 3.43 sec to 3.35 sec, settling-time is dwindled from 3.61 sec to 3.52 sec, steady-state-error is dwindled from 3.78 RPM to 2.66 RPM. Table 6 outlines the time domain parameters for torque with reference speed of 1350 RPM using CM-PI and CM-FOPID controller. By using CM-FOPID controller, rise-time is dwindled from 3.38 sec to 3.36 sec, peak-time is dwindled from 3.45 sec to 3.40 sec, settling-time is dwindled from 3.83 sec to 3.71 sec, Steady-state-error is dwindled from 0.70 to 0.61 N-m.

Table 7 outlines the time domain parameters for speed of 1400 RPM using CM-PI and CM-FOPID controller. By using CM-FOPID controller, rise-time is dwindled from 3.25 sec to 3.24 sec, peak-time is dwindled from 3.38 sec to 3.29 sec, settling-time is dwindled from 3.57 sec to 3.45 sec, steady-state-error is dwindled from 3.62 RPM to 2.76 RPM. Table 8 outlines the time domain parameters for torque with reference speed of 1400 RPM using CM-PI and CM-FOPID controller. By using CM-FOPID controller, rise-time is dwindled from 3.35 Sec to 3.33 sec, peak-time is dwindled from 3.39 sec to 3.37 sec, settling-time is dwindled from 3.75 sec to 3.69 sec and steady-state-error is dwindled from 0.68 to 0.52 N-m.

By using CM-FOPID (motor speed), rise-time, peak-time and steady-state-error are reduced. By using CM-FOPID (motor torque), rise-time, peak-time and steady-state-error are also reduced. Hence, the outcome indicates that the closed loop PV-QBC-GZSI-IMS with CM-FOPID is superior to closed loop PV-QBC-GZSI-IMS with CM-PI controller.

Table 3. Comparison time domain parameters of motor speed 1300 rpm

Type of controller	Tr	Tp	Ts	Ess (Rpm)
CM-PI	3.28	3.46	3.68	3.98
CM-FOPID	3.27	3.38	3.56	2.85

Table 4. Comparison time domain parameters of motor torque for 1300 rpm

Type of controller	Tr	Tp	Ts	Ess (N-m)
CM-PI	3.39	3.48	3.89	0.76
CM-FOPID	3.37	3.45	3.76	0.65

Table 5. Comparison time domain parameters of motor speed 1350 rpm

Type of controller	Tr	Tp	Ts	Ess (Rpm)
CM-PI	3.27	3.43	3.61	3.78
CM-FOPID	3.26	3.35	3.52	2.66

Table 6. Comparison time domain parameters of motor torque at 1350 rpm

Type of controller	Tr	Tp	Ts	Ess (N-m)
CM-PI	3.38	3.45	3.83	0.70
CM-FOPID	3.36	3.40	3.71	0.61

Table 7. Comparison time domain parameters of motor speed 1400 rpm

Type of controller	Tr	Tp	Ts	Ess (Rpm)
CM-PI	3.25	3.38	3.57	3.62
CM-FOPID	3.24	3.29	3.45	2.76

Table 8. Comparison time domain parameters of motor torque at 1400 rpm

Type of controller	Tr	Tp	Ts	Ess (N-m)
CM-PI	3.35	3.39	3.75	0.68
CM-FOPID	3.33	3.37	3.69	0.52

6. CONCLUSION

This paper has analyzed closed loop QBC-GZSIS. It is suitable for induction motor drive that integrates PV-system. Further, the reduced response time makes it appropriate to use it for systems with higher band-width. Combination of QBC&GZSI is proposed for control of IM. Speed regulation of closed loop-PV-QBC-GZSI-IMS for pumps with CM-PI and CM-FOPID controller are simulated with MATLAB/Simulink platform. The simulation-outcomes of Speed and torque time domain comparison in closed-loop-PV-QBC-GZSI-IMS with-CM-PI and CM-FOPID controllers are presented. By using CM-FOPID (motor speed), rise-time, peak-time and steady-state-error are reduced. By using FOPIDC, settling-time of speed is reduced to 3.45 sec, steady-state-error in speed is reduced to 2.76 RPM. By using CM-FOPID, rise-time, peak-time and steady-state-error are also reduced. Hence, the outcome illustrates that the closed loop CM-FOPID controlled PV-QBC-GZSI-IMS is superior to closed loop CM-PI controller. PV-QBC-GZSI-IMS has high voltage gain and reduced ripple. Fast time response is achieved by using CMC for PV-QBC-GZSI-IMS. The drawback of PV-QBC-GZSI-IMS is that it uses large number of passive elements for QBC and GZSI. The characteristics of QBC-GZSI fed induction motor matches with the characteristics of pump. Combination of QBC-GZSI is identified as a suitable converter inverter system for induction motor drive. FOPID controlled PV-QBC-GZSI-IMS is found to have improved response compared to PI controlled PV-QBC-GZSI-IMS. The present work improves the time response of PV-QBC-GZSI-IMS using the current mode - FOPID controller. By using QBC and GZSI, we can also reduce the PV rating of the panel.

Performance of closed-loop PV-QBC-GZSI-IMS with CM-PI and CM-FOPID controller is investigated here. Closed-loop PV-QBC-GZSI-IMS with CM-PR and hysteresis controller can be done in

future. Efficiency of PV-QBC-GZSI-IMS can be improved by replacing normal diodes and MOSFETs with silicon carbide devices.

ACKNOWLEDGEMENT




Major thanks are to the vice chancellor and Head of the department of Sathyabama Institute of Science and Technology, Chennai, India for providing facilities to conduct simulation studies. The authors would like to mention that they have not received any fund from any agency.

REFERENCES




- [1] P. S. Gnanamurthy and V. Govindasamy, "Analysis of cascaded H-bridge multilevel inverter with current control methods," *International Journal of Power Electronics and Drive Systems*, vol. 13, no. 2, pp. 998–1006, 2022, doi: 10.11591/ijpeds.v13.i2.pp998-1006.
- [2] C. T. Manikandan and G. T. Sundarajan, "Fuzzy logic controller for closed loop cascaded flyback converter fed pmc motor system," *International Journal of Power Electronics and Drive Systems*, vol. 11, no. 4, pp. 1857–1865, 2020, doi: 10.11591/ijpeds.v11.i4.pp1857-1865.
- [3] M. A. George, D. V. Kamat, and C. P. Kurian, "Electronically Tunable ACO Based Fuzzy FOPID Controller for Effective Speed Control of Electric Vehicle," *IEEE Access*, vol. 9, pp. 73392–73412, 2021, doi: 10.1109/ACCESS.2021.3080086.
- [4] M. G. Ortiz-Lopez, J. Leyva-Ramos, E. E. Carbajal-Gutierrez, and J. A. Morales-Saldana, "Modelling and analysis of switch-mode cascade converters with a single active switch," *IET Power Electronics*, vol. 1, no. 4, pp. 478–487, 2008, doi: 10.1049/iet-pel:20070379.
- [5] J. Leyva-Ramos, J. M. Lopez-Cruz, M. G. Ortiz-Lopez, and L. H. Diaz-Saldierna, "Switching regulator using a high step-up voltage converter for fuel-cell modules," *IET Power Electronics*, vol. 6, no. 8, pp. 1626–1633, 2013, doi: 10.1049/iet-pel.2012.0433.
- [6] O. Lopez-Santos, L. Martinez-Salamero, G. Garcia, H. Valderrama-Blavi, and T. Sierra-Polanco, "Robust sliding-mode control design for a voltage regulated quadratic boost converter," *IEEE Transactions on Power Electronics*, vol. 30, no. 4, pp. 2313–2327, 2015, doi: 10.1109/TPEL.2014.2325066.
- [7] J. Viola, L. Angel, and J. M. Sebastian, "Design and robust performance evaluation of a fractional order PID controller applied to a DC motor," *IEEE/CAA Journal of Automatica Sinica*, vol. 4, no. 2, pp. 304–314, 2017, doi: 10.1109/JAS.2017.7510535.
- [8] Y. Tang, S. Xie, C. Zhang, and Z. Xu, "Improved Z-source inverter with reduced Z-source capacitor voltage stress and soft-start capability," *IEEE Transactions on Power Electronics*, vol. 24, no. 2, pp. 409–415, 2009, doi: 10.1109/TPEL.2008.2006173.
- [9] Y. R. Kafle, S. Ul Hasan, and G. E. Town, "Quasi-Z-source based bidirectional DC-DC converter and its control strategy," *Chinese Journal of Electrical Engineering*, vol. 5, no. 1, pp. 1–9, 2019, doi: 10.23919/CJEE.2019.000001.
- [10] F. Z. Peng, "Z-Source inverter for motor drives," *PESC Record - IEEE Annual Power Electronics Specialists Conference*, vol. 1, pp. 249–254, 2004, doi: 10.1109/pesc.2004.1355750.
- [11] A. Narendran and R. Sureshkumar, "Hysteresis-controlled - landsman converter based multilevel inverter fed induction-motor system using PIC," *Microprocessors and Microsystems*, vol. 76, 2020, doi: 10.1016/j.micpro.2020.103099.
- [12] A. Hota and V. Agarwal, "Novel Three-Phase H10 Inverter Topology with Zero or Constant Common-Mode Voltage for Three-Phase Induction Motor Drive Applications," *IEEE Transactions on Industrial Electronics*, vol. 69, no. 7, pp. 7522–7525, 2022, doi: 10.1109/TIE.2021.3097656.
- [13] M. A. Hernandez Navas, F. G. Lozada, J. L. Azcua Puma, J. A. A. Torrico, and A. J. Sguarez Filho, "Battery Energy Storage System Applied to Wind Power System Based on Z-Source Inverter Connected to Grid," *IEEE Latin America Transactions*, vol. 14, no. 9, pp. 4035–4042, 2016, doi: 10.1109/TLA.2016.7785930.
- [14] S. Bayhan, H. Abu-Rub, and R. S. Balog, "Model Predictive Control of Quasi-Z-Source Four-Leg Inverter," *IEEE Transactions on Industrial Electronics*, vol. 63, no. 7, pp. 4506–4516, Jul. 2016, doi: 10.1109/TIE.2016.2535981.
- [15] F. Guérin, D. Lefebvre, A. B. Mboup, J. Y. Paréde, E. Lemains, and P. A. S. Ndiaye, "Hybrid modeling for performance evaluation of multisource renewable energy systems," *IEEE Transactions on Automation Science and Engineering*, vol. 8, no. 3, pp. 570–580, 2011, doi: 10.1109/TASE.2011.2140317.
- [16] P. C. Loh, D. Li, and F. Blaabjerg, "T-Z-Source Inverters," *IEEE Transactions on Power Electronics*, vol. 28, no. 11, pp. 4880–4884, Nov. 2013, doi: 10.1109/TPEL.2013.2243755.
- [17] Y. Zhou, H. Li, and H. Li, "A single-phase PV quasi-Z-source inverter with reduced capacitance using modified modulation and double-frequency ripple suppression," *IEEE Transactions on Power Electronics*, vol. 31, no. 3, pp. 2166–2173, 2016, doi: 10.1109/TPEL.2015.2432070.
- [18] Y. Asadi, A. Ahmadi, S. Mohammadi, A. M. Amani, M. Marzband, and B. Mohammadi-Ivatloo, "Data-driven model-free adaptive control of z-source inverters," *Sensors*, vol. 21, no. 22, 2021, doi: 10.3390/s21227438.
- [19] C. A. Ramos-Paja, D. Gonzalez Montoya, and J. D. Bastidas-Rodríguez, "Sliding-mode control of a CuK converter for voltage regulation of a dc-bus," *Sustainable Energy Technologies and Assessments*, vol. 42, 2020, doi: 10.1016/j.seta.2020.100807.
- [20] K. Aseem and S. Selva Kumar, "A PWM-based Sliding Mode Control Scheme for Isolated Solar Photovoltaic Systems," *Journal of The Institution of Engineers (India): Series B*, vol. 103, no. 2, pp. 313–328, 2022, doi: 10.1007/s40031-021-00649-8.
- [21] A. Goudarzian, A. Khosravi, and N. R. Abjadi, "Input-output current regulation of Zeta converter using an optimized dual-loop current controller," *Electrical Engineering*, vol. 102, no. 1, pp. 279–291, 2020, doi: 10.1007/s00202-019-00872-z.
- [22] S. Shaikh, D. Kumar, A. Hakeem, and A. M. Soomar, "Protection System Design of Induction Motor for Industries," *Modelling and Simulation in Engineering*, vol. 2022, 2022, doi: 10.1155/2022/7423018.
- [23] Q. T. Tran and V. Q. Nguyen, "Reduction of common mode voltage for grid-connected multilevel inverters using fuzzy logic controller," *International Journal of Power Electronics and Drive Systems*, vol. 14, no. 2, pp. 698–707, 2023, doi: 10.11591/ijpeds.v14.i2.pp698-707.
- [24] S. W. Shneen and A. L. Shurajji, "Simulation model for pulse width modulation-voltage source inverter of three-phase induction motor," *International Journal of Power Electronics and Drive Systems*, vol. 14, no. 2, pp. 719–726, 2023, doi: 10.11591/ijpeds.v14.i2.pp719-726.
- [25] M. Zerouali, A. El Ougli, and B. Tidhaf, "A robust fuzzy logic PI controller for solar system battery charging," *International Journal of Power Electronics and Drive Systems*, vol. 14, no. 1, pp. 384–394, 2023, doi: 10.11591/ijpeds.v14.i1.pp384-394.

BIOGRAPHIES OF AUTHORS






Krishnan Selvaraj    received his BE in Electrical and Electronics Engineering from Anna University, Chennai, India in 2011. He finished his ME in Power Electronics and Drives from Anna University, Chennai, India in 2013. Currently he is pursuing his Ph.D. degree in Electrical and Electronics Engineering from Sathyabama Institute of Science and Technology, Chennai, India. His research interest includes converter, inverters, power electronics and its applications in renewable energy. He can be contacted at email: krishna05me@gmail.com.



Anbarasi Jebaselvi Gnanaiah David    has completed her BE in Government College of Engineering, Tirunelveli, in 1990 and pursued her ME in College of Engineering, Guindy, Anna University and obtained her Master's degree in 2003. She received the Ph.D. degree from Sathyabama Institute of Science and Technology, Chennai, India. She is currently working in Sathyabama Institute of Science and Technology, Chennai, India. Her research interest includes renewable energy sources particularly wind and solar systems, modeling of wind electric generators, solar power technologies and power electronic converters. She has published around 25 papers including many Scopus indexed ones and one of the papers appeared in a high rated journal viz. Elsevier. Her research findings have been explicit through her paper presentations and publications in various international conferences and journals. She can be contacted at email: gdjebaselvianbarasi16@gmail.com.



Rama Reddy Sathi    received his DEE from S.M.V.M Polytechnic, Tanuku, A.P., AMIE in Electrical Engineering from the Institution of Engineers (India), ME in Power System Anna University. He received the PhD degree in the area of Resonant Converters from College of Engineering, Anna University, Chennai. He is currently working in Rajalakshmi Engineering College, Chennai, India. He has published 30 Technical papers in National and International Conference proceeding/Journals. He has secured AMIE Institution Gold medal for obtaining higher marks. He has secured AIMO best project award. He has worked with Tata Consulting Engineers, Bangalore and Anna University, Chennai. His research interest is in the area of the micro-grids and converters for E-vehicles. He is a life member of Institution of Engineers (India), Indian Society for India and Society of Power Engineers. He is a fellow of Institution of Electronics and Telecommunication Engineers (India). He has published books on power electronics and solid-state circuits and electromagnetic fields. He can be contacted at email: ramareddy.s@rajalakshmi.edu.in.



Pradeepa Kuppusamy    received her BE in Electrical and Electronics Engineering from Anna University, Chennai, India in 2011. She completed her ME in Power Electronics and Drives from Anna University, Chennai, India in 2013. Currently she is working in Rajalakshmi Engineering College, Chennai, India. Her research interest includes converter, inverters, power electronics and its applications in renewable energy. She can be contacted at email: pradeepakrishnaneee@gmail.com.